

LIQUID CRYSTAL LATTICE MODELS I. BULK SYSTEMS

PAOLO PASINI, CESARE CHICCOLI
Istituto Nazionale di Fisica Nucleare, Sezione di Bologna
Via Irnerio 46, 40126, Bologna, ITALY

AND

CLAUDIO ZANNONI
Dipartimento di Chimica Fisica ed Inorganica, Università di
Bologna
Viale Risorgimento 4, 40136, Bologna, ITALY

Abstract. Monte Carlo simulations of spin models for liquid crystal bulk systems are described. A concise description of second rank Lebwohl-Lasher models of various dimensionality and of models containing in addition interactions of first and fourth rank is provided. Biaxial lattice models are also briefly discussed.

1. Introduction

Lattice spin models consist of systems of interacting centres (“spins”) placed at the sites of a certain regular lattice. The spins can be thought of as idealized unit vectors assuming discrete or continuously varying orientations in a space of given “spin dimensionality” s . The lattice of positions will have its own, possibly different, dimensionality d . Classical examples are the Ising and Heisenberg models [1] that have played and still play a key role in the study of magnetism. Indeed, despite their simplicity, spin models have proved to be extremely important in the study of phase transitions and critical phenomena in many fields of physics ranging from liquids to polymers [1, 3, 2]. Although lattice systems with their intrinsic positional order are in some sense the very antithesis of liquid crystals, they have also been successfully employed in investigating nematics since the pioneering work of Lebwohl and Lasher (LL) [4]. In this case the spins that represent

the molecules or groups of molecules should possess full rotational freedom, rather than a discrete set of orientations, so as not to affect the long range orientational behavior. A large amount of work has been and is currently done on generalizations of the LL hamiltonian even though in the last few years more realistic potentials with full translational freedom, like the Gay-Berne one [5], have become increasingly popular thanks also to the continuous increase in computing power. It is, in any case, fair to say that as long as the properties of interest are purely orientational, there are several advantages in using simple lattice models, with respect to potentials with translational freedom, the foremost of which is probably the possibility of performing simulations on a larger (often $10^2 - 10^3$ times larger!) number of particles while conserving the essence of the physics. As an alternative, when using smaller lattices, it is possible to investigate potentials for relatively complicated systems depending on additional parameters, for example associated with varying boundary conditions and field strengths, over a wide range of state points.

Here we wish to present and briefly review some lattice models of bulk liquid crystals and their computer simulations to show how these simple potentials can be useful in investigating the orientational properties of nematics.

2. Periodic boundary conditions

Before going into the details of the various models we wish to mention the ubiquitous problem of the choice of boundary conditions, i.e. of what to surround the simulated sample with. Tackling it is unavoidable since computer simulations are usually performed on a relatively limited number of particles N . Even for lattice models N is of the order of $10^3 - 10^6$ in comparison with a bulk system for which the interacting particles are of the order of the Avogadro number. Then, apart from choosing a lattice size as large as possible, it is very important to adopt some artifact at the sample surfaces so as to minimize the effects of the finite size of the system. The appropriate choice of the boundary conditions becomes then essential especially when small systems are investigated.

The most often used boundary conditions are the so called periodic ones (PBC), where the sample box is surrounded by exact replicas of itself (see Fig. 1). Although this kind of boundary conditions introduces a non existent periodicity and thus some spurious correlation, PBC effectively reduce the effect of the finite size and of the sample surfaces. Due to the greater correlation between sites it is expected that periodic boundary conditions will overestimate the transition temperature T_C . The opposite case arises when the correlation between sites is underestimated as in the case of free

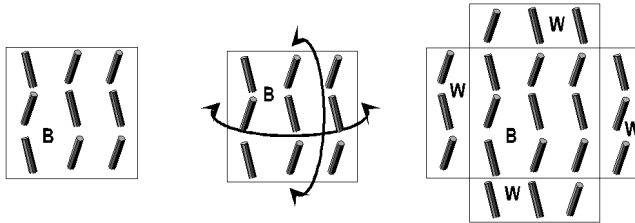


Figure 1. A schematic representation of boundary conditions in a 2D lattice system: empty or free (left), periodic (middle) and cluster (right).

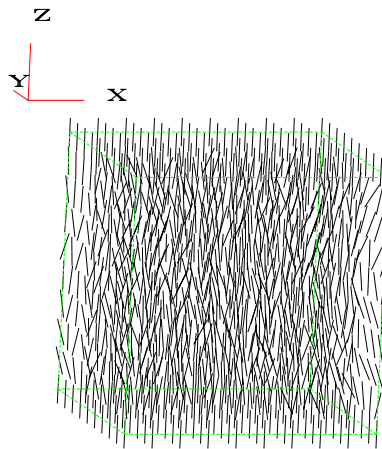


Figure 2. The LL lattice model in the nematic phase.

boundary surfaces. Consequently periodic and free boundaries should give, respectively, an upper and a lower bound for the transition temperature:

$$T_C(\text{free}) < T_C < T_C(\text{periodic}), \quad (1)$$

and this has been checked at least for 2d lattices [6]. In any case PBC represent the standard approach to simulating bulk phases and we shall adopt it here, although we shall see later that other and sometimes more effective approaches can also be employed.

3. The Lebwohl-Lasher model

The prototype lattice model for modelling liquid crystals was devised many years ago by Lebwohl and Lasher (LL) [4] and is the simplest one with the correct symmetry for nematics (in particular the potential is invariant for an head-tail flip of the molecules). The particles, assumed to have uniaxial

symmetry and represented by three dimensional spins located at the sites of a $L \times L \times L$ cubic lattice (see Fig. 2), interact through a pair potential of the form:

$$U_{ij} = -\epsilon_{ij}P_2(\cos \beta_{ij}), \quad (2)$$

where ϵ_{ij} is a positive constant, ϵ , for nearest neighbour spins i and j and zero otherwise, P_2 is the second Legendre polynomial and β_{ij} is the angle between the molecules. The interaction tends to bring molecules parallel to one another and effectively models whatever underlying intermolecular interaction either attractive or repulsive that does that. The model has been studied [7, 8, 9, 10, 11, 12] and generalized by many authors [14, 15, 13, 16] and we shall see later a few relevant examples.

3.1. OBSERVABLES

While Monte Carlo computer simulations of LC lattice models typically proceed following the standard Metropolis [17] procedure (see Chapter 1) two issues require special attention and will be covered here starting with the LL model: one is the determination of phase transitions and the other the calculation of orientational order and other anisotropic observables.

3.1.1. *Energy and heat capacity*

The phase transition of the model is located by monitoring as a function of temperature the constant volume specific heat defined as:

$$C_V^* = \partial U^* / \partial T^*, \quad (3)$$

and obtained by a numerical differentiation of energy with respect to temperature [7]. We use the star for dimensionless variables, e.g. $T^* = kT/\epsilon$ with k the Boltzmann constant.

This is a only seemingly simple task since numerical differentiation typically requires smoothing and this in turn masks the transition. Indeed at times the derivative is best calculated solving an integral equation! [18] The specific heat can also be calculated from the energy fluctuations:

$$C_V^*/k = (\langle U^{*2} \rangle - \langle U^* \rangle^2) / (kT^*)^2, \quad (4)$$

although this tends to be somewhat noisy.

The dimensionless energy per particle of a system with N spins, $U^* = \langle U \rangle / N\epsilon$, is in turn calculated by the sum:

$$U^* = \frac{1}{N(N-1)\epsilon} \sum_{i=1}^N \sum_{j=i+1}^N U_{ij}. \quad (5)$$

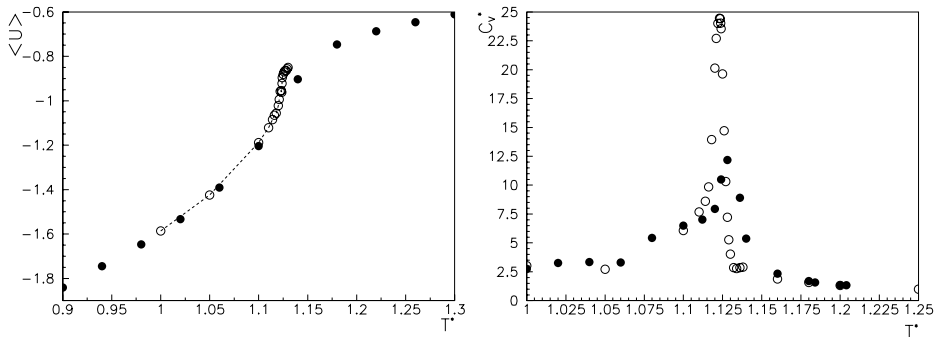


Figure 3. The single particle energy U^* (left) and heat capacity C_V^* (right) vs dimensionless temperature $T^* = kT/\epsilon$ for the Monte Carlo simulation of a $10 \times 10 \times 10$ (full circles) and a $30 \times 30 \times 30$ (empty circles) [9] Lebwohl-Lasher systems.

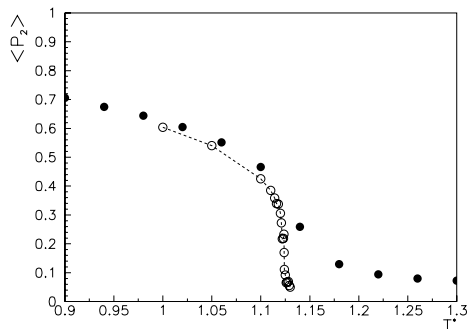


Figure 4. The second rank order parameter $\langle P_2 \rangle$ vs dimensionless temperature $T^* = kT/\epsilon$ as obtained from MC simulations on a $10 \times 10 \times 10$ (full circles) and a $30 \times 30 \times 30$ (empty circles) [9] LL systems.

For the LL system the values range then from $U^* = -3$ for a perfectly aligned system to $U^* = 0$ for an isotropic phase.

First order transitions are characterized by a singularity in the heat capacity in the thermodynamic limit. In a finite system, however, the transition region is broadened and the heat capacity just peaks at a phase transition. Then C_V^* is used in locating the phase transition temperature T_c^* . For the LL model T_{NI}^* was determined [9] in this way to be $T_{NI}^* = 1.1232 \pm 0.0006$. Furthermore the maximum of the peak increases with the system size [19, 20, 22]:

$$C_V^{max}(L) = a + bL^3, \quad (6)$$

where a and b are size independent parameters.

The energy and the heat capacity variation with temperature as obtained from Monte Carlo simulations on two lattices with different sizes

with PBC can be seen in Figure 3. The peaks sharpens with the increase of L and actually scales as expected from (6). The first order character of the transition is confirmed also by an analysis of the distribution of energy values collected, as histograms, during the simulation runs, that shows the double peak behaviour expected for coexisting ordered and disordered states [21]. A more modern analysis [46] based on Ferrenberg and Swendsen [23] reweighting method confirms the results of [9].

3.1.2. Order parameters

The second rank orientational order parameter can be defined as :

$$\langle P_2 \rangle = \frac{1}{N} \sum_{i=1}^N P_2(\mathbf{u}_i \cdot \mathbf{n}), \quad (7)$$

where \mathbf{u}_i is the molecular axis of the i -th particle and \mathbf{n} the director. However, in these Monte Carlo simulations there is no external field applied to pin the director and \mathbf{n} can change during the system evolution. A description of the determination of the order parameters in computer simulations is reported in Chapter 2 of this book. Here we recall only that the problem of determining the order parameter reduces to that of finding the unit vector \mathbf{n} which renders the order in a certain configuration $\langle P_2 \rangle_S$ a maximum and this in turn amounts to calculating and diagonalizing the ordering matrix \mathbf{Q} defined as:

$$\mathbf{Q} = \frac{1}{2N} \sum_{i=1}^N 3u_{i\alpha}u_{i\beta} - \frac{1}{2}\delta_{\alpha\beta}, \quad (8)$$

with $u_{i\alpha}$ the direction cosines of the i -th molecule, and identifying the order in the S configuration $\langle P_2 \rangle_S$ with its largest eigenvalue [7]. The eigenvalues of a matrix are scalars, independent on an overall frame rotation and thus on the orientation of the instantaneous director \mathbf{n} with respect to the laboratory frame. Then a global average, $\langle P_2 \rangle_\lambda$, can be obtained by first calculating the order parameter by diagonalization of \mathbf{Q} at each desired configuration and then averaging over a sufficiently large number of configurations. A related procedure has been given for $\langle P_4 \rangle_\lambda$ in ref. [9]. The second rank order parameters obtained in this way from the simulations of two LL lattice systems are shown in Figure 4. As mentioned before the LL model reproduces rather well the temperature dependence of the order parameter versus temperature observed in real nematics, that can normally be written as:

$$\langle P_2 \rangle = (1 - T/T_{NI})^\beta + \langle P_2 \rangle_{iso} \quad T < T_{NI}. \quad (9)$$

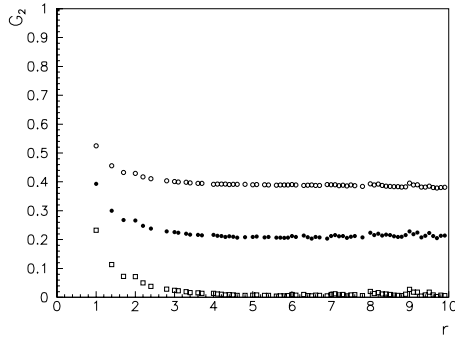


Figure 5. The second rank orientational correlation function G_2 vs distance r as obtained from MC simulations on a $10 \times 10 \times 10$ LL systems. The results are for $T^* = 1.0$ (upper curve), $T^* = 1.1$ (middle curve) and $T^* = 1.2$ (bottom curve),

In fact it has been found that the exponent ranges approximately from 0.17 up to 0.25 for a large series of both Schiff base and cyanobiphenyl nematics [24, 25] while the LL model gives 0.22 ± 0.01 [16]. In real experiments $\langle P_2 \rangle_{iso} = 0$ while for the finite samples used in simulations $\langle P_2 \rangle_{iso} \approx O(\sqrt{N})$.

This behavior can be obtained also using small lattices (a few thousand spins) and possibly the model works so well because a “spin” can be thought to represent, rather than a single particle, a closely packed group of molecules, that maintains its local structure at various temperatures and even across the nematic/isotropic phase transition [26]. As a special case these domains could comprise just one molecule but it seems more realistic to assume that they typically include a few tens of particles [27].

3.1.3. Orientational correlation functions

While $\langle P_2 \rangle$ and the higher $\langle P_L \rangle$ offer a description of the orientational long range order in the case it exists, the problem of deciding if true long range order does indeed exist remains to be tackled and orientational correlation functions $G_L(r)$ are particularly useful to this effect. The set of correlations $G_L(r)$ can be defined as expansion coefficients of the rotationally invariant pair distribution [7]:

$$G(r, \beta_{12}) = G_0^{00}(r) \sum_L \frac{2L+1}{64\pi^2} G_L(r) P_L(\cos \beta_{12}). \quad (10)$$

$G_0^{00}(r)$ is the particle centre distribution that, for a cubic lattice, is just:

$$G_0^{00}(r) = \frac{1}{4\pi\rho r^2} \sum_k z_k \delta(r - r_k), \quad (11)$$

where ρ is the density and z_k the number of neighbours at r_k . Thus $G_L(r)$ are a sort of two particle order parameters, which give the correlation between the orientations of two particles separated by a distance r :

$$G_L(r) = \langle P_L(\cos \beta_{12}) \rangle_r, \quad (12)$$

where $\langle \dots \rangle_r$ is a normalized average over all spins falling in a thin spherical shell centred at r and of width corresponding to the chosen resolution Δ .

The pair coefficients $G_L(r)$ should start from one and tail off to essentially $\langle P_L \rangle^2$ [7]. Thus we expect $G_L(r)$ to decay to a plateau only if long range order exists, as in the nematic phase. As we can gather from the above formulas the calculation runs on particle pairs and can be quite time consuming when the size of the lattice is large, representing a relevant percentage of the total time spent in the simulation. Usually the first two angular pair correlation coefficients G_2 and G_4 are calculated.

In fig. 5 we show $G_2(r)$ at some selected temperature below and above the phase transition for the LL model.

3.2. LOW DIMENSIONAL SYSTEMS

Low dimensional systems present interesting and challenging problems such as the very existence and nature of their phase transitions and have received a lot of interest from many authors [28, 29, 30, 31, 32, 33, 34]. We notice that the planar LL model is of interest also from a purely theoretical point of view to test the existence of topological phase transitions in non-abelian two dimensional systems [35, 36].

We here consider systems with reduced space dimensionality: $d = 2$ and $d = 1$, while keeping $s = 3$, in other words a planar and a linear LL lattice where molecules can still reorient in three dimensions.

Looking at the heat capacity behavior of the $d = 2$ lattice as a function of size it is clear from the simulation results that the scenario is very different in comparison with the 3D system and that in particular the heat capacity is insensitive to the increase in the number of particles as can be seen in Fig. 6 where the results for four increasing sizes are shown.

Although no true phase transition is expected in a two dimensional LL system [37] the heat capacity anomaly divides the temperature range in two regions which shows a different behavior in the decay of orientational pair correlation function (Fig. 7 *left*). The analysis of these quantities [30]

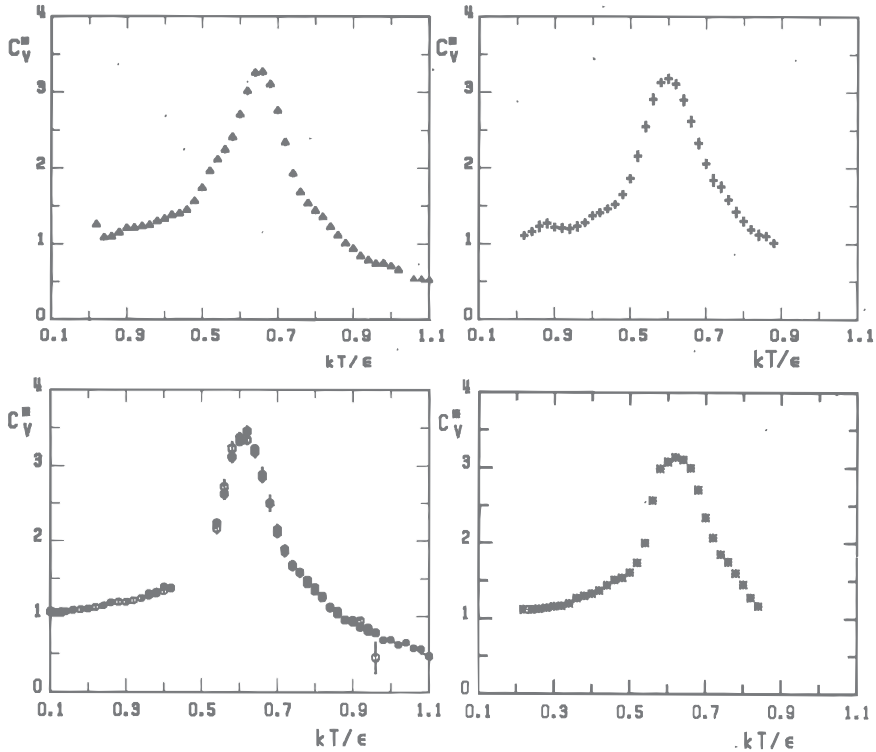


Figure 6. The heat capacity C_V^* obtained from differentiation of energy plotted versus dimensionless temperature $T^* = kT/\epsilon$ for the Monte Carlo simulations of four size planar Lebwohl-Lasher systems, i.e. 10×10 (top left), 20×20 (top right), 60×60 (bottom left) and 80×80 (bottom right).

indicates that a power law decay of the type:

$$G_2(r) = A_p/r^{k_p} \quad (13)$$

is the best fit for the simulation data in the ordered phase while an exponential decay:

$$G_2(r) = (1 - A_e)e^{-k_e r} + A_e \quad (14)$$

describes the correlation function behavior above the pseudo-transition temperature. Thus the planar system can present large ordered domains for $T^* < T_c^*$ but not for $T^* > T_c^*$.

To conclude this short overview of space dimensionality effects it is interesting to look now at a one dimensional, $d = 1$, $s = 3$ lattice. This 1D system is constituted by a chain of particles which are free to rotate in a 3D space. An analytical solution for this model, given by Vuillermot and Romerio [38], exists and shows that no phase transition occurs and that the

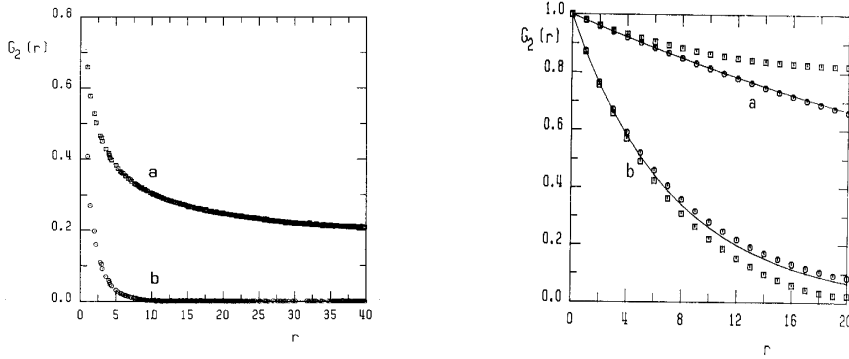


Figure 7. The second rank orientational correlation function G_2 versus distance r (lattice units) at two selected temperatures, i.e. below (a) and above (b) the heat capacity anomaly. *Left:* G_2 for the planar LL model. *Right:* G_2 for the monodimensional case for $L = 40$ (squares) and $L = 100$ (circles) compared with the analytic solution [38] (lines).

system is ordered only at zero temperature (see Fig. 8). It is instructive

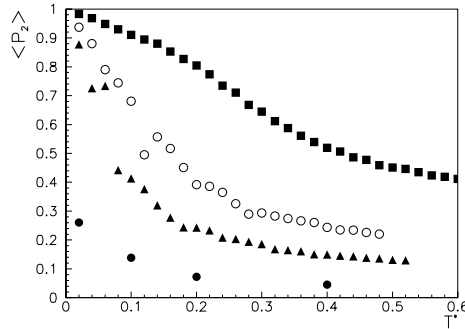


Figure 8. The second rank order parameter $\langle P_2 \rangle$ vs dimensionless temperature $T^* = kT/\epsilon$ for a 1D LL system of various lengths: $L=10$ (squares), $L=40$ (empty circles), $L=100$ (triangles), $L=1000$ (full circles).

to see that $\langle P_2 \rangle$ can be quite misleading as an indicator of the existence of true long range order, especially if a size dependent study is not performed (Fig. 8). On the contrary a fit of $G_2(r)$ reveals very clearly the exponential decay of orientational correlations [31] (Fig. 7 *right*).

In summary we see that the different behavior of $G_2(r)$ can help in assessing the presence and particularly the absence of long range order.

3.3. CLUSTER BOUNDARY CONDITIONS

Although quite satisfactory when far from a phase transition, the use of periodic boundary conditions (PBC) leads to large smearing and broadening of the heat capacity and order parameter vs. temperature curves. This complicates the location of the transition and demands the use of very large samples. There is therefore an interest in looking for alternative schemes and, for instance, another type of boundary condition was proposed within the Cluster Monte Carlo (CMC) method [39]. In this approach the simulation sample is surrounded by an additional layer of particles (*ghosts*) which have on average the same properties as the particles inside. In the CMC method, the desired bulk or global average of a quantity A is written as an average over all the external “world” configurations $[W]$ of the values $\langle A \rangle_{[W]}$ calculated for a fixed configuration of the “world” outside the sample box [39]. Thus the global average is

$$\langle A \rangle_G = \langle \langle A \rangle_{[W]} \rangle_W \quad (15)$$

$$\approx (1/M_W) \sum_{[W]} \langle A \rangle_{[W]}. \quad (16)$$

In practice a MC simulation is run to obtain $\langle A \rangle_{[W]}$ and the outside world configurations needed are obtained by creating a layer of ghost particles outside the sample box having the same one-particle distribution of the system inside the box. The orientations of the virtual neighbours are sampled from an orientational distribution function constructed, using maximum entropy principles,[40] from the order parameters calculated inside the sample, i.e.

$$P(\cos \beta) = \exp\left[\sum_{L=0}^{L'} a_L P_L(\cos \beta)\right], \quad (17)$$

where the coefficients a_L are determined from the constraint that the available $\langle P_L \rangle$ can be reobtained by averaging $P_L(x)$ over the distribution. For example $\langle P_2 \rangle$ and $\langle P_4 \rangle$ have been used for the LL model, and the coefficients a_2, a_4 have been determined by solving the non linear system

$$\langle P_L \rangle = \frac{\int_0^\pi d\beta \sin \beta P_L(\cos \beta) \exp[a_2 P_2(\cos \beta) + a_4 P_4(\cos \beta)]}{\int_0^\pi d\beta \sin \beta \exp[a_2 P_2(\cos \beta) + a_4 P_4(\cos \beta)]}, \quad L = 2, 4 \quad (18)$$

During the simulation the order parameters $\langle P_2 \rangle$, $\langle P_4 \rangle$ inside the sample are calculated and a_2 and a_4 are determined. The orientations for the ghost particles outside the box are then sampled from the distribution

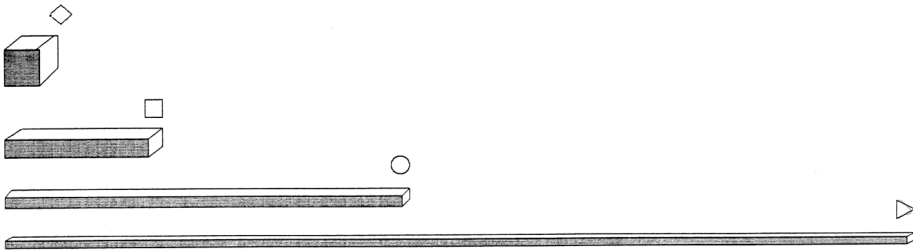


Figure 9. The various shape systems with similar volume, i.e., from top to bottom: $10 \times 10 \times 10$, $5 \times 5 \times 40$, $3 \times 3 \times 110$ and $2 \times 2 \times 250$.

in Eq. 18, the energy of the system is then recalculated and evolution proceeds. In the subsequent cycles the order parameters with respect to the Z laboratory direction P_L^J for the spins inside the box are still calculated. After a certain number of cycles M an average is calculated for this K trajectory segment together with the attendant standard deviation σ_K . These $\langle P_2 \rangle_{in}$ and $\langle P_4 \rangle_{in}$ parameters are then compared to the ones outside and if the difference is statistically significant a new set of orientations for the ghost molecules is generated using the new order parameters. The other parts of the Monte Carlo simulation method and particularly lattice updates proceed as usual. A more detailed description of the method is given in [39].

The method, that avoids the spurious correlations between particles separated by more than half the box size, has been successfully tested for various lattice models [39, 13, 41, 42] where it has given results comparable with those obtained employing PBC on lattices up to 2^d times larger in d dimensional systems. The CMC boundaries are particularly useful when potentials with one or more additional parameters have to be studied and a set of independent simulations has to be performed to obtain a phase diagram [13] as we shall show later on.

3.4. SAMPLE SHAPE

Another possibly significant advantage in using non-periodic CMC boundaries is the complete freedom over the shape of the sample that it allows us to simulate, for example, spherical samples [42, 16] and that different shapes with similar N can be used without affecting the results. Since computer simulations are numerical experiments performed on finite and rather

small systems with the aim of reproducing the bulk it is to be hoped that the simulations should not depend very significantly on the sample size and shape: indeed these are accessories to the calculation not relevant in a truly bulk sample. Ideally the choice of the boundary conditions should ensure that the size and the shape employed do not affect the behavior of the system under study. On the other hand employing Periodic Boundary Conditions in non cubic systems may give results very different from a bulk behavior [43], as we can see from the results of simulations performed on LL systems of very different shapes [43] (see Fig. 9), containing approximately the same number of spins (Figs.10 and 11) We see that changing the shape of the sample the results show a pronounced variation for PBC but not for CMC. Upon decreasing the breadth and width of the sample while keeping the volume constant, the system tends to approach, using PBC, the limit of one dimensional model (cf. Fig. 9). Also the second rank order parameter results confirm that PBC tends to induce a one dimensional behavior increasing the length to breadth ratio of the sample and, in this latter case $\langle P_2 \rangle$ (see Fig. 11 *left plate*) can be compared with the 1D simulation data (Fig. 8).

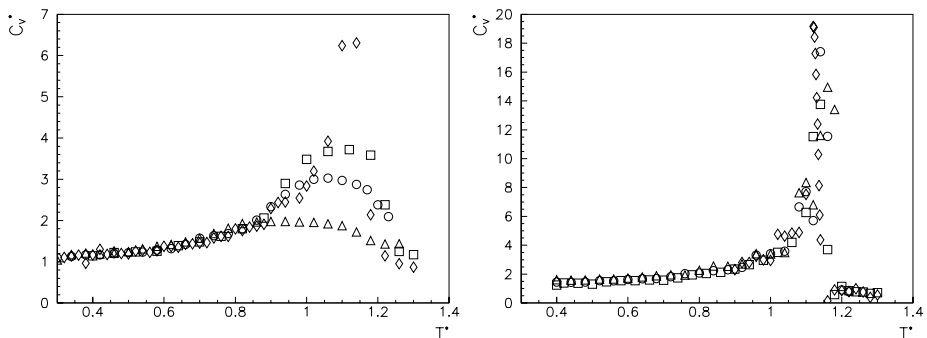


Figure 10. The heat capacity C_V versus dimensionless temperature $T^* = kT/\epsilon$ as obtained from PBC (left) and CMC (right) simulations of LL systems with different shapes, i.e. $2 \times 2 \times 250$ (squares), $3 \times 3 \times 110$ (empty circles), $5 \times 5 \times 40$ (triangles) and $10 \times 10 \times 10$ (full circles).

4. Some other nematic lattice spin models

The simplicity of lattice models allows to study in detail potentials depending on more than one relevant parameter. In these cases the simulation has to be repeated for various values of these physical parameters and the determination of transition temperatures and transition behavior implies a challenging exercise in computer simulations [2, 1, 39]. The choice of boundary conditions like the CMC ones is of considerable importance because a

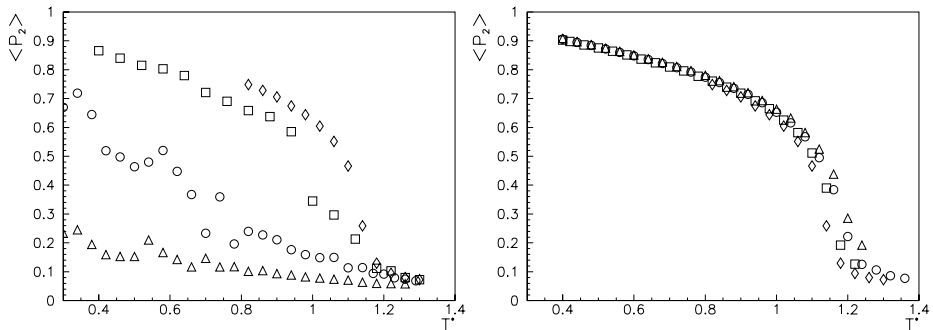


Figure 11. The second rank order parameter $\langle P_2 \rangle$ vs. dimensionless temperature $T^* = kT/\epsilon$ as obtained from PBC (left) and CMC (right) simulations of LL systems with different shapes. System sizes and symbols are as in Fig. 9.

large number of simulations can be performed using smaller lattices in order to obtain a phase diagram for the model. Here we consider two examples involving generalizations of the LL model.

4.1. A P_2P_4 MODEL

As mentioned above the temperature dependence of the orientational order for the LL model is in quite a good agreement with the experimental results for nematics. However, it is interesting to examine the effects of a fourth rank contribution, easily the first neglected term in a general expansion of the pair interaction and examine how strictly the observed experimental results are related to the specific second rank nature of the potential. A fourth rank contribution has often been invoked in interpreting experimental results in nematics [44] and in membrane vesicles [45] and some simulation studies of the mixed P_2P_4 interaction potential have been performed [14, 16, 46].

The P_2P_4 hamiltonian can be written as:

$$U_{ij} = -\epsilon_{ij}[P_2(\mathbf{u}_i \cdot \mathbf{u}_j) + C_4P_4(\mathbf{u}_i \cdot \mathbf{u}_j)] \quad ; \quad \text{with } i \neq j, \quad (19)$$

where C_4 designates the relative strength of the interactions. A three dimensional representation of the potential as a function of β_{ij} and C_4 (Fig. 12) shows how the location of the potential minima changes with the fourth rank contribution. The MC simulation results for the specific heat for various values of C_4 are reported in Fig. 13. We see that the fourth rank term has a profound effect on the transition. A positive contribution shifts T_{NI}^* to higher temperature and makes the transition much more pronouncedly first order, while a negative C_4 has the opposite effect, weakening the transition and shifting it to a lower temperature.

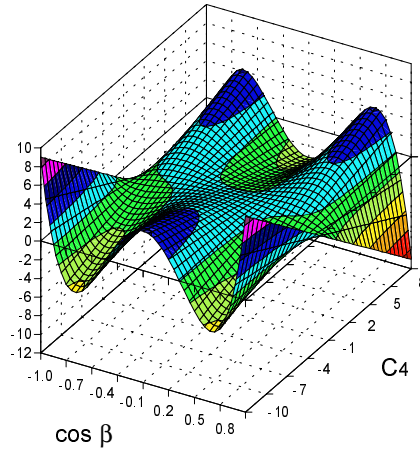


Figure 12. A plot of the P_2P_4 potential between two spins as a function of their relative orientation $\cos \beta = \mathbf{u}_i \cdot \mathbf{u}_j$ for various fourth rank contributions C_4 .

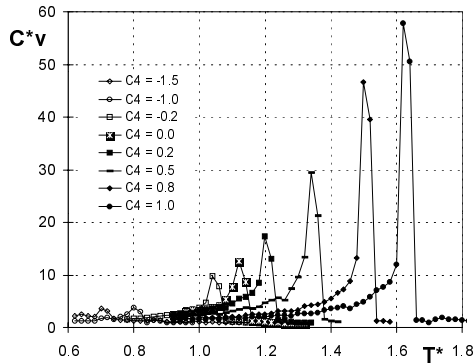


Figure 13. Heat capacity $C_V^* \equiv C_V/k$ dependence on reduced temperature $T^* \equiv kT/\epsilon$ for various values of C_4 as obtained from MC simulation on an approximate spherical lattice with Cluster boundary conditions. The lines are a guide for the eye.

The order parameter versus reduced temperature curve (Fig. 14) shows that a fourth rank contribution can vary the effective exponent β in eq. 9 and that only a limited range of C_4 can yield a β value compatible with experiment.

4.2. A P_1P_2 MODEL

Another interesting mixed rank potential contains a simple combination of first and second rank interactions proposed by Krieger and James [47]

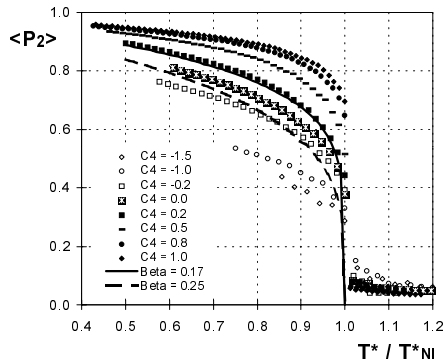


Figure 14. The second rank order parameter $\langle P_2 \rangle$ dependence on scaled temperature $T^+ \equiv T^*/T_{NI}^*$ for various values of C_4 . The continuous curves denote the region limited by the experimental exponents β in the Haller law as obtained for real liquid crystals.

and later by Lin Lei [48]. The first rank term simulates the head - tail asymmetry and the potential can be viewed as a prototype model for bowlic and ferroelectric liquid crystals. The hamiltonian reads:

$$U_{ij} = -\epsilon_{ij}[P_2(\cos \beta_{ij}) + \xi P_1(\cos \beta_{ij})], \quad (20)$$

where the parameter ξ determines the relative importance of the first rank term (Heisenberg model) with respect to the second one (Lebwohl-Lasher model), while its sign determines ferroelectric or antiferroelectric type interactions. Realization of a molecular system with ferroelectric type ordering is actively sought and could be made possible by a combination of steric and dipolar interactions as, e.g., in pyramidic systems [49, 50].

The simulations [13] confirm the Mean Field predictions [47] about the phase diagram, shown in Fig. 15, with three phases: polar, nematic and isotropic. In the polar phase (P) both the first and the second rank order parameters, $\langle P_1 \rangle$ and $\langle P_2 \rangle$ respectively, are non zero. In the nematic region (N) $\langle P_1 \rangle$ is zero while, as usual, $\langle P_2 \rangle$ survives and both of them vanish in the isotropic phase (I). The tricritical point occurs at a value of $\xi = 0.3578$.

4.3. A BIAXIAL MODEL

In all the lattice models presented above, as in the large majority of theoretical calculations and computer simulations of liquid crystals, the mesogenic molecules are assumed to be cylindrically symmetric. However it is important to recall that nematogen molecules are invariably not cylindrically symmetric and that a much more realistic approximation is to treat them at

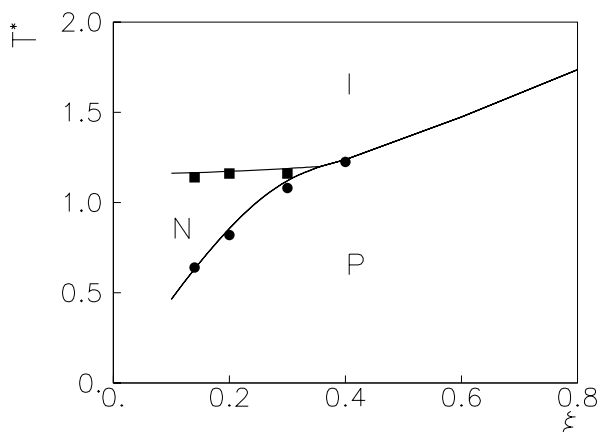


Figure 15. The P_1P_2 model phase diagram showing the reduced transition temperature versus the relative strength parameter ξ . The simulations results (points) are reported together with the Two Site Cluster predictions (curves).

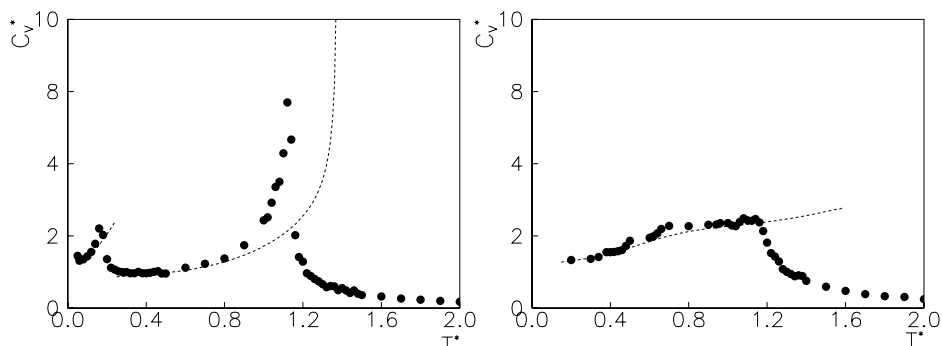


Figure 16. The heat capacity C_V^* versus temperature for two different molecular biaxialities, i.e. $\lambda = 0.2$ (left) and $\lambda \approx 1/\sqrt{6}$ (right). The results are from the simulations (dots) and MF Theory (lines).

least as biaxial objects. Ordered phases formed by biaxial particles have indeed been studied using a number of theoretical methods: Mean Field Theory (MFT) [51, 52, 53, 54, 55], counting methods [56], Landau-deGennes theory [57], bifurcation analysis [58, 59]. Both attractive interactions and hard particle models have been investigated. It should be stressed that typical nematic phases have uniaxial symmetry around the preferred direction, the director, even if the constituent molecules are themselves biaxial. However, the possibility of a biaxial nematic mesophase has been predicted by all these studies. The existence of this phase has also been confirmed by Monte Carlo simulations of a lattice system of biaxial particles [15, 60] and

of a fluid system of biaxial spherocylinders [61]. A simple lattice model of a biaxial system is described by the second rank attractive pair potential:

$$U(\omega_{ij}) = -\epsilon_{ij}\{P_2(\cos \beta_{ij}) + 2\lambda[R_{02}^2(\omega_{ij}) + R_{20}^2(\omega_{ij})] + 4\lambda^2 R_{22}^2(\omega_{ij})\}, \quad (21)$$

where λ is the biaxiality parameter that accounts for the deviation from cylindrical molecular symmetry: when λ is zero, the biaxial potential reduces to the Lebwohl - Lasher P_2 potential, while for λ different from zero the particles tend to align not only their major axis, but also their short axis. $\omega \equiv (\alpha, \beta, \gamma)$ is the set of Euler angles specifying the orientation of a molecule. The potential depends on the relative orientation ω_{ij} of the molecular pair, R_{mn}^L are combinations of Wigner functions symmetry - adapted for the D_{2h} group of the two particles:

$$R_{00}^2 = \frac{3}{2} \cos^2 \beta - \frac{1}{2} \quad (22)$$

$$R_{20}^2 = \frac{1}{2} \sqrt{\frac{3}{2}} \sin^2 \beta \cos 2\alpha \quad (23)$$

$$R_{02}^2 = \frac{1}{2} \sqrt{\frac{3}{2}} \sin^2 \beta \cos 2\gamma \quad (24)$$

$$R_{22}^2 = \frac{1}{4} (\cos^2 \beta + 1) \cos 2\alpha \cos 2\gamma - \frac{1}{2} \cos \beta \sin 2\alpha. \quad (25)$$

The model has been studied on a fcc lattice by Luckhurst and Romano for $\lambda = 0.2$ [15] and on a cubic lattice for a fairly large set of biaxialities by Chiccoli et al. [62]. The largest value for λ , $\lambda = \frac{1}{\sqrt{6}}$, separates the region of distorted rods from that of distorted disks that can be mapped into one another [52]. This means that for $\lambda > \frac{1}{\sqrt{6}}$, that is for discotic molecules, one can change the y and z axes of the molecules and use the potential with the corresponding $\lambda' < \frac{1}{\sqrt{6}}$ and ϵ' . In other words for $\lambda > \frac{1}{\sqrt{6}}$ there is a mapping of the system to another system with $\lambda < \frac{1}{\sqrt{6}}$, and all the thermodynamic results should be the same (of course the temperature $T = kT/\epsilon$ will correspond to $T' = kT/\epsilon'$).

The simulations has proved very useful in investigating the thermodynamics of this biaxial model and improving the Mean Field Theory prediction. At low values of biaxiality two transitions occur as clearly visible from the two peaks in the heat capacity curve (see Fig. 16), peaks which coalesce approaching the $\lambda = \frac{1}{\sqrt{6}}$, self dual, case. The phase diagram, obtained from a set of MC simulations at various molecular biaxiality is shown in Fig. 17 together with the MFT prediction. The lower transition lines identify the biaxial - nematic phase transition and have a second order character. The upper curve denotes the nematic isotropic phase transition: it is first order for low values of the molecular biaxiality and becomes more second order approaching the dual point. This uniaxial-isotropic transition highlights some differences between MC and MFT. In fact, while the MFT

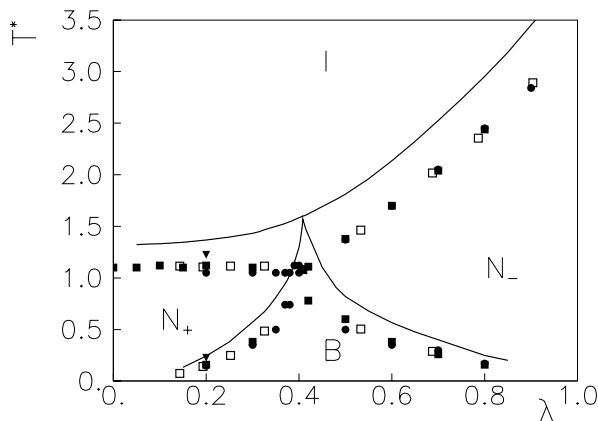


Figure 17. The biaxial model phase diagram showing the reduced transition temperature versus molecular biaxiality λ . The points are simulation results while the continuous curves are the mean field predictions. The tricritical point corresponds to a value $\lambda = 1/\sqrt{6}$ [60].

curve increases with λ the MC results are nearly constant or even show an opposite behavior. This could be relevant in understanding the difficulties in observing a true thermotropic nematic which would be competing in real systems with potential smectic or crystal phases. If, as observed in [63] the typical range of a nematic is of the order of 10% from T_{NI} then the MC phase diagram shows that the biaxial region (B) accessible to experiments is reduced further at lower temperatures and at higher values of λ with respect to the MFT expectations.

The simulations have also been used to calculate the biaxial order parameters. A method to obtain the order parameters is described in Chapter 2 of the present book where a full set of this second rank quantities is also presented. The availability of these biaxial data has allowed other researchers to calculate elastic constants for the model [64].

5. Conclusions

Computer simulations of lattice spin models for liquid crystals have been around for many years but still offer interesting opportunities for investigating anisotropic materials. Their simplicity allows to easily modify the models by adding terms that try to keep into account various effects such as contributions of different rank and symmetry. In particular they are useful in studying phase transitions, transition temperatures and collective properties to a precision not too lower than experiment something that requires in turn very large simulation sample sizes. They have also revealed useful in studying relatively small lattices under a variety of different conditions

to investigate confined nematic liquid crystals as we shall see in the next Chapter.

Acknowledgments

We thank MURST, CNR, University of Bologna, INFN (grant I.S. BO12) for support and our coworkers over many years, particularly F. Biscarini and F. Semeria.

References

1. Binder, K.(ed.), (1984) *Applications of the Monte Carlo Method in Statistical Physics* (Springer - Verlag).
2. Allen, M.P. and Tildesley, D.J. (1987) *Computer Simulation of Liquids*, Clarendon Press, Oxford.
3. Kremer, K. and Binder, K. (1988) *Computer Phys. Rep.*, **7**, 259.
4. Lebwohl, P.A. and Lasher G., (1972) *Phys Rev. A*, **6**, 426.
5. Gay, J.G. and Berne, B.J. (1981) *J. Chem. Phys.*, **74**, 3316.
6. Binder, K., (1974) *Adv. Phys.*, **23**, 917.
7. Zannoni, C., (1979) in: *The Molecular Physics of Liquid Crystals*, eds. Luckhurst, G.R. and Gray, G.W., ch. 9. Academic Press, New York.
8. Luckhurst, G.R. and Simpson, P., (1982) *Mol. Phys.*, **47**, 251.
9. Fabbri, U. and Zannoni, C., (1986) *Molec. Phys.*, **58**, 763.
10. Zhang, Z., Zuckermann, M.J. and Mouritsen, O.G., (1991) *Phys. Rev. Lett.*, **69**, 2803.
11. Cleaver, D.J. and Allen, M.P., (1991) *Phys. Rev. A*, **43**, 1918.
12. Greef, C.W. and Lee, M.A., (1994) *Phys. Rev. E*, **49**, 3225.
13. Biscarini, F., Zannoni, C., Chiccoli, C. and Pasini, P., (1991) *Molec. Phys.*, **73**, 439.
14. Fuller, G.J., Luckhurst, G.R. and Zannoni, C. (1985) *Chem. Phys.*, **92**, 105.
15. Luckhurst, G.R. and Romano, S. (1980) *Mol. Phys.*, **40**, 129.
16. Chiccoli, C., Pasini, P. and Zannoni, C., (1997) *Int. J. Mod. Phys. B.*, **11**, 1937.
17. Metropolis N., Rosenbluth A.W., Rosenbluth M.N., Teller A.H. and Teller E., (1953) *J. Chem. Phys.*, **21**, 1087.
18. Chiccoli, C., Pasini, P., and Zannoni, C., (1987) *Liq. Cryst.*, **2**, 39.
19. Fisher, M.E. (1971) in *Proceedings of the International School E. Fermi*, Course 51, Varenna, Green, M.S. (ed), Academic, New York.
20. Binder, K. and Landau, D.P. (1984) *Phys. Rev. B*, **30**, 1477.
21. Mouritsen, O.G. (1984), *Computer Studies of Phase Transitions and Critical Phenomena* Springer, Berlin.
22. Zhang, Z., Mouritsen, O. G. and Zuckermann, M. (1993) *Mod. Phys. Lett. B*, **7**, 217.
23. Ferrenberg A.M. and Swendsen, R.H. (1988) *Phys. Rev. Lett.*, **61**, 2635.
24. Leenhouts, F. , de Jeu, W.H. and Dekker, A.J. (1979) *J. de Physique*, **40**, 989.
25. Wu, S.T. and Cox, R.J. (1988) *J. Appl. Phys.*, **64**, 821.
26. Luckhurst, G.R. and Zannoni, C. (1977) *Nature*, **267**, 412.
27. Berggren, E., Chiccoli, C., Pasini, P., Semeria, F. and Zannoni, C. (1994) *Phys. Rev. E*, **50**, 2929.
28. Mountain, R. and Rujgrok, Th.W. (1977) *Physica*, **89A**, 522.
29. Tobochnik, J. and Chester, G.V. (1979) *Phys. Rev B*, **20**, 3761.
30. Chiccoli, C., Pasini, P., and Zannoni, C., (1988) *Physica*, **148A**, 298.
31. Chiccoli, C., Pasini, P., and Zannoni, C., (1988) *Liq. Cryst.*, **3**, 363.
32. Romano, S. (1987) *Nuovo Cim.*, **B100**, 447.
33. Romano, S. (1988) *Nuovo Cim.*, **D10**, 1459.

34. Romano, S. (1991) *Liq. Cryst.*, **10**, 73.
35. Kunz, H and Zumbach, G., (1991) *Phys. Lett.* , **257B**, 299.
36. Caracciolo, S., Edwards, R.G., Pellissetto, A. and Sokal, A.D. (1993) *Nucl. Phys. B (Proc. Suppl.)*, **30**, 815.
37. Vuillermot, P.A. and Romerio, M.V. (1975) *Commun. Math. Phys.*, **41**, 281.
38. Vuillermot, P.A. and Romerio, M.V. (1973) *J. Phys. C*, **6**, 2922.
39. Zannoni, C., (1986) *J. Chem. Phys.*, **84** , 424.
40. Levine, R.D. and Tribus, M. (eds.) (1979) *The Maximum Entropy Formalism* MIT Press, Boston.
41. Chiccoli, C. , Pasini, P., Biscarini, F., Zannoni, C. (1988) *Molec. Phys.*, **65**, 1505.
42. Chiccoli, C., Pasini, P., Semeria, F. and Zannoni, C. (1993) . *Int. J. Mod. Phys. C*, **4**, 1041.
43. Chiccoli, C., Pasini, P., Semeria, F. and Zannoni, C., (1993) *Phys. Lett. A*, **176**, 428.
44. Pottel, H., Herreman, W., van der Meer, B.W. and Ameloot, M. (1986) *Chem. Phys.*, **102**, 37.
45. Ameloot, M., Hendrickx, H., Herreman, W., Pottel, H., van Cauwelaert, F. and van der Meer, W. (1984) *Biophys. J.*, **46**, 525.
46. Zhang, Z., Zuckermann, M. and Mouritsen, O. G. *Mol. Phys.* (1993), **80**, 1195.
47. Krieger, T.J. and James, H.M., (1954) *J. Chem. Phys.*, **22** , 796.
48. Lin Lei, (1987) *Mol. Cryst. Liq. Cryst.*, **146** , 41.
49. Malthête, J. and Collet, A., (1985) *Nowv. J. de Chimie*, **9** , 151.
50. Zimmermann, H., Poupko, R., Luz, Z. and J. Billard, (1985) *Z.Naturforsch.*, **40a** , 149.
51. Freiser, M.J. (1970) *Phys. Rev. Lett.*, **24**, 1041.
52. Straley, J.P. (1974) *Phys. Rev. A*, **10**, 1881.
53. Luckhurst, G.R., Zannoni, C., Nordio, P.L., Segre, U. (1975) *Mol. Phys.*, **30**, 1345.
54. Priest, R.G. (1975) *Solid State Comm.*, **17**, 519.
55. Remler, D.K. and Haymet, A.D.J. (1986) *J. Phys. Chem.*, **90**, 5426.
56. Shih, C.S. and Alben, R. (1972) *J. Chem. Phys.*, **57**, 3055.
57. Gramsbergen, E.F., Longa, L. and de Jeu, W.H. (1986) *Phys. Reports*, **135**, 195.
58. Mulder, B.M. (1986) *Liq. Cryst.*, **1**, 539.
59. Holyst, R. and Ponierewski, A. (1990) *Mol. Phys.*, **69**, 193.
60. Biscarini, F., Chiccoli, C., Pasini, P., Semeria, F., and Zannoni, C. (1995) *Phys. Rev. Lett.*, **75**, 1803.
61. Allen, M.P. (1990) *Liq. Cryst.*, **8**, 499.
62. Chiccoli, C., Pasini, P., Semeria, F., and Zannoni, C. (1999) *Int. J. Mod. Phys. C*, **10**, 469.
63. Ferrarini A., Nordio P.L., Spolaore E. and Luckhurst G.R., (1995) *J. Chem. Soc. Faraday Trans.*, **91**, 3177.
64. Longa L., Stelzer J. and Dunmur D., (1998), *J. Chem. Phys.*, **109**, 1555.

Table of Contents

5	LIQUID CRYSTAL LATTICE MODELS I.	
	BULK SYSTEMS	99
1	Introduction	99
2	Periodic boundary conditions	100
3	The Lebwohl-Lasher model	101
3.1	Observables	102
3.2	Low dimensional systems	106
3.3	Cluster boundary conditions	108
3.4	Sample shape	110
4	Some other nematic lattice spin models	111
4.1	A P_2P_4 model	112
4.2	A P_1P_2 model	113
4.3	A biaxial model	114
5	Conclusions	117